

- FORTIER, S. & HAUPTMAN, H. (1977). *Acta Cryst.* **A33**, 694–696.  
 GIACOVAZZO, C. (1974). *Acta Cryst.* **A30**, 522–524.  
 GIACOVAZZO, C. (1975). *Acta Cryst.* **A31**, 252–259.  
 GIACOVAZZO, C. (1976). *Acta Cryst.* **A32**, 91–99.  
 GIACOVAZZO, C. (1979). *Acta Cryst.* **A35**, 296–305.  
 GIACOVAZZO, C. (1980). *Direct Methods in Crystallography*. London: Academic Press.  
 GRADSHTEYN, I. & RYZHIK, I. (1980). *Table of Integrals, Series, and Products*. New York: Academic Press.  
 HAUPTMAN, H. (1974). *Acta Cryst.* **A30**, 822–829.  
 HAUPTMAN, H. (1975). *Acta Cryst.* **A31**, 671–679.  
 HAUPTMAN, H. & GREEN, E. A. (1978). *Acta Cryst.* **A34**, 216–223.  
 HAUPTMAN, H. & KARLE, J. (1953). *Acta Cryst.* **6**, 136–141.  
 HEINERMAN, J. J. L. (1977). *Acta Cryst.* **A33**, 100–106.  
 HEINERMAN, J. J. L., KRABBENDAM, H. & KROON, J. (1977). *Acta Cryst.* **A33**, 873–878.  
 HEINERMAN, J. J. L., KRABBENDAM, H. & KROON, J. (1979). *Acta Cryst.* **A35**, 101–103.  
 KARLE, J. & HAUPTMAN, H. (1958). *Acta Cryst.* **11**, 264–269.  
 KLUG, A. (1958). *Acta Cryst.* **11**, 515–543.  
 NAYA, S., NITTA, I. & ODA, T. (1965). *Acta Cryst.* **19**, 734–747.  
 PESCHAR, R. & SCHENK, H. (1986). *Acta Cryst.* **A42**, 309–317.  
 SHMUELI, U. & WEISS, G. H. (1985). *Acta Cryst.* **A41**, 401–408.  
 TSOUCARIS, G. (1970). *Acta Cryst.* **A26**, 492–499.  
 WATSON, G. N. (1942). *A Treatise on the Theory of Bessel Functions*, 2nd ed. Cambridge Univ. Press.

*Acta Cryst.* (1987). **A43**, 393–400

## Diffraction Patterns from Tilings with Fivefold Symmetry

BY E. PRINCE

*Institute for Materials Science and Engineering, National Bureau of Standards, Gaithersburg, Maryland 20899, USA*

(Received 21 March 1986; accepted 1 December 1986)

### Abstract

A procedure involving projection from six-dimensional to three-dimensional space to describe objects that give sharp diffraction with fivefold symmetry can be reduced to the easier problem of projection from two dimensions to one dimension. This result is used to derive an explicit formula for the quasilattice contribution to the diffracted intensity for an arbitrary size and shape of the selection region. The predictions of this formula are compared with the electron diffraction patterns obtained from rapidly solidified aluminium–manganese alloys, and it is concluded that the edges of the rhombic faces of the three-dimensional objects from which models for these alloy structures may be constructed is larger than that used in previous analyses by a factor of  $\tau^3$ , where  $\tau$  is the golden mean. It is shown that the quasilattice density is proportional to the volume of the selection region in the complementary three-dimensional space into which a lattice point in six-dimensional space must project in order for the point to be included in the direct space; this results in important constraints on the possible structures of these alloys.

### Introduction

The recent discovery by Shechtman, Blech, Gratias & Cahn (1984) of electron diffraction patterns with icosahedral symmetry that have sharp spots has stimulated a new study of the conditions under which such diffraction patterns may exist. Sharp diffraction has traditionally been associated with periodic lat-

tices, and it has long been known that fivefold rotation symmetry is incompatible with an infinite translation lattice. It has been shown, however (Levine & Steinhardt, 1984), that sharp diffraction does occur from non-periodic patterns under some conditions. Moreover, as was first shown by Penrose (1974; also Mackay, 1976; Gardner, 1977), patterns with fivefold symmetry can be produced that have long-range order although they lack periodicity. The two-dimensional Penrose tilings have been generalized to three dimensions by Mackay (1981, 1982). [In fact, Mackay's results were anticipated by Baer (1970), who used the principles to construct a number of interesting architectural structures.] Kramer & Neri (1984), Duneau & Katz (1985) and Kalugin, Kitayev & Levitov (1985) have shown that the three-dimensional tilings can be understood in terms of projection from six dimensions, in which fivefold rotation is compatible with periodicity, into three dimensions.

Regardless of whether the alloy of aluminium and manganese that was studied by Shechtman *et al.* (1984) is actually an example of a three-dimensional object that has an inherent icosahedral diffraction pattern, the mathematical development of the diffraction properties of these tilings stands by itself, independent of its applications to any experimental observations. As in periodic crystals, the intensity of a diffraction spot for the 'quasicrystal' (Mackay, 1981) with fivefold symmetry is proportional to the product of two factors, one due to the projected lattice and one due to the arrangement of atoms associated with each point. In contrast to crystals, however, the spots

in the diffraction patterns of quasicrystals correspond to points in reciprocal space that have different weights, and the structure cannot be reproduced by the repeat of a single unit. The purpose of this paper is to present a simple formula for the weights of the reciprocal quasilattice points and to discuss conditions that must be satisfied by possible structures. Because the previous mathematical development is extremely fragmented, it is necessary to begin with a brief review of the results we shall use.

### The golden mean and Fibonacci numbers

We shall first summarize some mathematical relations that are associated with fivefold symmetry. The Fibonacci numbers may be defined by  $F_n = [\tau^n - (-1/\tau)^n]/\sqrt{5}$ , where  $\tau = 2 \cos(\pi/5) = (1 + \sqrt{5})/2$ . It is readily verified from this formula that  $F_0 = 0$ ,  $F_1 = 1$  and  $F_{n+1} = F_n + F_{n-1}$ , from which it follows that the Fibonacci numbers form a sequence of integers each of which is the sum of the two that precede it in the sequence.  $\tau$  is known as the 'golden mean' and is the positive root of the quadratic equation  $x^2 - x - 1 = 0$ . Because  $F_{n-1} = F_{n+1} - F_n$ , the Fibonacci numbers are defined for negative as well as positive values of  $n$ , and it is also readily verified from the definition that  $\tau^n = F_{n-1} + F_n\tau$ , and that  $\lim_{n \rightarrow \infty} F_{n+1}/F_n = \tau$ . Particularly important relations are  $\tau^2 = \tau + 1$  and  $1/\tau = \tau - 1$ .

### The Fourier transform of a one-dimensional non-periodic sequence

Levine & Steinhardt (1984) showed that a particular one-dimensional non-periodic sequence would show sharp diffraction. If one uses the properties of the Fibonacci numbers, the fact that such a sequence gives sharp diffraction may be shown as follows:

Consider an array of points along a line such that the displacement of the  $n$ th point from the origin is given by

$$x_n = n + [n/\tau](\tau - 1), \quad (1)$$

where  $[y]$  designates 'the largest integer less than or equal to  $y$ '. This defines a sequence of segments of length either 1 or  $\tau$ . There are never two consecutive segments with length 1, there may be either one or two segments with length  $\tau$ , and over a long range the ratio of the number of segments with length 1 to the number of segments with length  $\tau$  approaches 1: $\tau$ . This sequence will have a weighted average spacing equal to  $(1 + \tau^2)/(1 + \tau) = 1 + 1/\tau^2 = 3 - \tau$ . Defining a set of periods

$$a_m = (1 + 1/\tau^2)/\tau^m, \quad (2)$$

thereby defining a set of one-dimensional lattices  $L_m$ , and defining a deviation of  $x_n$  from a point in  $L_m$ ,

$$\Delta_{mn} = (nF_{m+1} + [n/\tau]F_m)a_m - x_n, \quad (3)$$

we can show that  $\Delta_{mn}$  is bounded and can be made arbitrarily small. First we multiply both sides of (3) by  $\tau^m$ , giving

$$\tau^m \Delta_{mn} = (nF_{m+1} + [n/\tau]F_m)a_0 - x_n\tau^m, \quad (4)$$

which, upon substitution for  $x_n$  [(1)] and use of  $1/\tau = \tau - 1$ , can be written

$$\begin{aligned} \tau^m \Delta_{mn} &= n(F_{m+1} - \tau^m) + (n/\tau)(\tau - 1)F_{m+1} \\ &\quad + [n/\tau](F_m + F_m/\tau^2 - \tau^{m-1}). \end{aligned} \quad (5)$$

With the expression for  $\tau^m$  in terms of the Fibonacci numbers, straightforward algebraic manipulation yields  $F_{m+1} - \tau^m = -F_m/\tau$ , and  $F_m + F_m/\tau^2 - \tau^{m-1} = F_{m+2} - F_{m+1}\tau$ . If we denote the quantity  $(n/\tau) - [n/\tau]$ , the 'fractional part of  $(n/\tau)$ ', by  $\{n/\tau\}$ , it follows that

$$\tau^m \Delta_{mn} \{n/\tau\} (F_{m+1}\tau - F_{m+2}), \quad (6)$$

which can also be written

$$\tau^m \Delta_{mn} = (-1)^m \{n/\tau\} / \tau^{m+1}. \quad (7)$$

Therefore

$$\Delta_{mn} = (-1)^m \{n/\tau\} / \tau^{2m+1}. \quad (8)$$

$\{n/\tau\}$ , by definition, lies in the range  $0 \leq \{n/\tau\} < 1$ , and, because  $\tau$  is irrational,  $\{n/\tau\}$  is uniformly distributed in this range as  $n$  takes all values from  $-\infty$  to  $+\infty$ . Thus, with respect to any period of the form  $a_m$  the point at  $x_n$  lies within a bounded region attached to some point in  $L_m$ , and the ensemble average of  $\Delta_{mn}$  for a large number of points  $x_n$  fills that bounded region uniformly. Furthermore,  $\lim_{m \rightarrow \infty} \Delta_{mn}/a_m = 0$ , so that the points  $x_n$  get closer and closer to fitting a periodic lattice.

Just as in a crystal in which the atoms undergo thermal vibrations, the array of points  $x_n$  may be replaced, for the purpose of computing the diffraction pattern, by the ensemble average contents of a unit cell of length  $a_m$ , except that the distribution is uniform, rather than Gaussian. The diffraction pattern is then given by the Fourier transform of the convolution of a uniform distribution whose range is the maximum value of  $|\Delta_{mn}|$  with a translation lattice of period  $a_m$ . The translation lattice leads to a Fourier transform with  $\delta$ -function peaks at points  $l/a_m$ , where  $l$  is an integer. The Fourier transform of the uniform distribution is

$$\begin{aligned} \Phi(q, t) &= (1/2\pi t) \int_{-\pi t}^{+\pi t} \exp(iqu) du \\ &= (1/2\pi t) \int_{-\pi t}^{+\pi t} \cos(qu) du, \end{aligned} \quad (9)$$

where  $t = 1/\tau^{2m+1}$ . The integral gives

$$\Phi(q, t) = \sin(\pi qt) / (\pi qt), \quad (10)$$

and the diffracted intensity, which is proportional to the square of the Fourier transform, is given by

$$I(q, t) = \delta(q - l/a_m) \sin^2(\pi qt)/(\pi qt)^2. \quad (11)$$

Because  $a_m$  is irrational the  $\delta$  functions fill the one-dimensional space densely, but for any finite positive number  $\varepsilon$  there is a finite number of points in any finite interval for which  $I(q) > \varepsilon$ . Therefore for any detection system where there is a discrete minimum of detectable intensity, the diffraction pattern will consist of sharp spots. Fig. 1 shows the features of this function as a function of  $q$ . For each value of  $l$  there is a sigmoid envelope that encloses sharp peaks at successive powers of  $\tau$ , corresponding to increasing values of  $m$ .

Levine & Steinhardt (1984) actually showed that  $\delta$ -function diffraction peaks would occur for all reciprocal-space points of the form  $m + m'\tau$ , not just those that can be expressed as an integral multiple of a power of  $\tau$ , for which  $m$  and  $m'$  are multiples of successive Fibonacci numbers. We shall see in a later section, however, that almost all spots with appreciable intensity fall in this special class.

#### Projection from two dimensions to one

The result derived algebraically in the previous section can also be derived geometrically (Zia & Dallas, 1985) by means of an irrational projection from two dimensions into one dimension. Referring to Fig. 2, consider a square lattice with a unit cell whose edge length is  $(1 + \tau^2)^{1/2}$  and a band through it with width  $w$  at an angle with the cell edge of  $\arctan(1/\tau)$ . If a lattice point lies within the band, that is if its projection on a line perpendicular to the band is less than  $w$ , it is projected onto the line marking the lower edge of the band. Because the projection line is an irra-

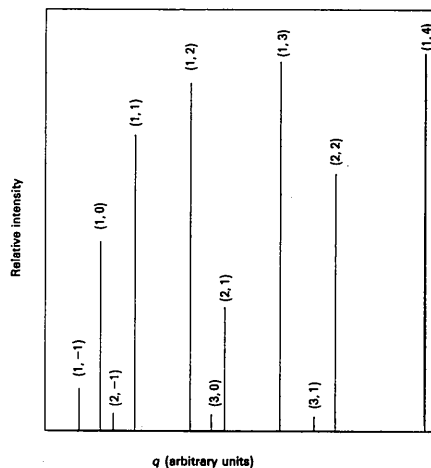


Fig. 1. Relative intensities for a one-dimensional non-periodic sequence of scattering centers. The indices  $(l, m)$ , as in equation (11), are shown.

tional direction in the square lattice, the pattern of projected points will never repeat. Nevertheless, any family of parallel lines with rational indices will intersect the projection line at a set of points that form a periodic one-dimensional lattice, and the projected points will always lie between the intersections of those lines with the two edges of the band. The Fibonacci sequence considered by Levine & Steinhardt (1984) corresponds to  $w = 1 + \tau$ , and Fig. 2 shows the construction with this width and the lines whose indices are  $(1, 1)$  which corresponds to  $l = 1$  and  $m = 0$ . The projected points never lie within the hatched region, but they may lie anywhere within the unhatched region.

If  $w = 1 + \tau$  all intervals in the projection will have length either 1 or  $\tau$ , but if  $w$  is slightly larger than  $1 + \tau$  there will be an occasional short interval of length  $\tau - 1$ . Similarly, if  $w$  is slightly smaller than  $1 + \tau$  there will be an occasional long interval with length  $\tau + 1$ . It is apparent that the average density of points over a long range in the one-dimensional space is proportional to  $w$ .

Because the lattice is square, its reciprocal lattice is also square. Designating the reciprocal-lattice coordinates by  $h$  and  $h'$  and the projections of the reciprocal-lattice points on the horizontal and vertical lines by  $r_x$  and  $r_y$ , we get the relations  $r_x = h + h'\tau$  and  $r_y = h' - h\tau$ . The thickness of the region within which the projected lattice points must fall is  $t = (r_y/r_x)w$ , and the period is  $d = 1/r_x$ . The diffracted intensity is proportional to  $\sin^2(\pi t/d)/(\pi t/d)^2$  or  $\sin^2(\pi r_y w)/(\pi r_y w)^2$ . In order for the relative intensity to be greater than  $(3\pi/2)^{-2}$ , the first subsidiary maximum of the  $\sin x/x$  function,  $r_y w$ , must be less than 1. In order for the density of the array of points to be positive,  $w$  must be a constant greater than 0, so that  $r_y$  should be as small as possible for large intensities. Because  $\lim_{m \rightarrow \infty} F_{m+1}/F_m = \tau$ , particularly

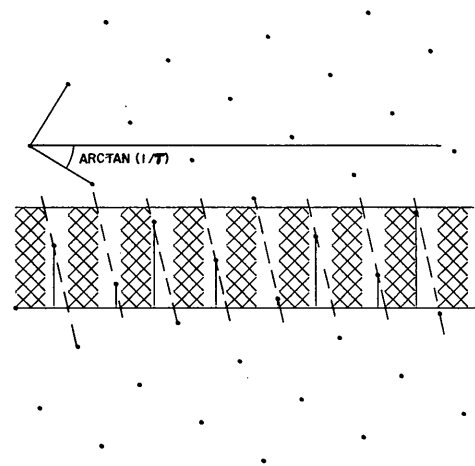


Fig. 2. Projection of a band in a two-dimensional square lattice, showing periodicity in a non-periodic sequence.

small values of  $r_y$ , occur when  $h$  and  $h'$  are successive Fibonacci numbers, so that the values of  $r_x$  are proportional to powers of  $\tau$ , in agreement with the algebraic result. The geometric model, however, makes it clear how to allow for arbitrary values of  $w$ , which becomes important when we come to consider the three-dimensional problem.

### The relation of structure to Penrose tiles

It is well known that fivefold rotation symmetry is incompatible with long-range periodicity. However, Penrose (1974) showed that with a combination of two suitably chosen shapes it was possible to tile a plane surface in such a way that there was complete long-range order, in the sense that the position of every vertex could be specified by a simple direct algorithm over an infinite range and fivefold symmetry about a single point in the pattern. Fig. 3 is an example of such a pattern in which the shapes are two rhombuses with acute angles of  $36^\circ$  and  $72^\circ$ . Gardner (1977) has described a number of interesting properties of this pattern. Although there can be fivefold symmetry that has infinite extent about one point only, finite-sized fivefold patterns of arbitrarily large size can be found around an infinite number of points. The ratio of the areas of the two rhombuses is  $1:\tau$ , and the average number density is also  $\tau$  of the large ones to one of the smaller ones, so that the area enclosed, like the line segments in the one-dimensional pattern, is in the ratio  $1:\tau^2$ . From the point of view of the diffraction properties an important feature of this pattern is that the vertices of the rhombus-shaped tiles lie on families of parallel lines with spacings in the ratio  $1:\tau$  in a non-periodic sequence that resembles the sequence that we have considered in previous sections. It has been shown (de Bruijn, 1981; Kramer & Neri, 1984) that a three-dimensional structure whose projection onto two

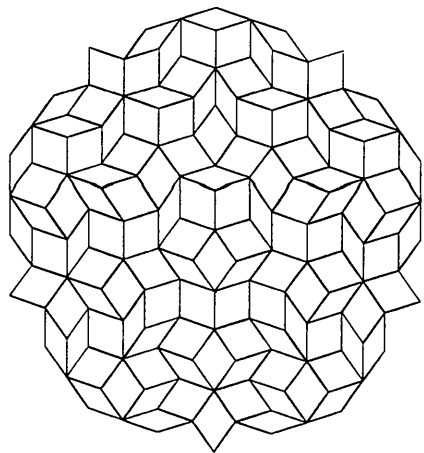


Fig. 3. A two-dimensional Penrose tiling with fivefold symmetry. The tiling has long-range order, but no periodicity.

dimensions resembled the Penrose tiles would have a diffraction pattern with five- or tenfold symmetry and a pattern of spacings and intensities similar to that shown in Fig. 1.

One way to construct such an object is with right prisms having the shapes of the tiles stacked periodically in the third dimension. One of the phases found in the rapidly solidified Mn-Al alloy appears to have just such a structure (Bendersky, 1985). The electron diffraction patterns observed by Shechtman *et al.* (1984), however, have icosahedral symmetry, so they cannot be due to an object that is periodic in any direction. We shall now discuss how an object with that sort of diffraction pattern can be constructed.

### Projection from six dimensions to three

Although icosahedral symmetry is incompatible with periodicity in three dimensions, it is easy to construct a representation of the icosahedral group,  $m\bar{3}5$ , that leaves a six-dimensional orthogonal isometric lattice, a 'hypercubic' lattice, invariant. This six-dimensional space may be projected into three-dimensional space so as to preserve the icosahedral symmetry in two ways, corresponding to the top three and bottom three rows of the matrix

$$P = \begin{pmatrix} \alpha & 0 & \alpha\tau & -\alpha & 0 & \alpha\tau \\ \alpha\tau & \alpha & 0 & \alpha\tau & -\alpha & 0 \\ 0 & \alpha\tau & \alpha & 0 & \alpha\tau & -\alpha \\ \alpha\tau & 0 & -\alpha & -\alpha\tau & 0 & -\alpha \\ -\alpha & \alpha\tau & 0 & -\alpha & -\alpha\tau & 0 \\ 0 & -\alpha & \alpha\tau & 0 & -\alpha & -\alpha\tau \end{pmatrix},$$

where  $\alpha = (1 + \tau^2)^{-1/2}$ . This matrix has a number of important properties. All rows and all columns are orthogonal. In addition the upper half of each column is orthogonal to the lower half, and each half of a row in the upper half is orthogonal to the same half of the corresponding row in the lower half. A unit vector along a coordinate axis in six dimensions projects to a unit vector normal to a face of the regular dodecahedron in each of the three-dimensional spaces. [This differs from the matrix defined by Cahn, Shechtman & Gratias (1986) in that their matrix transforms a unit vector along a coordinate axis in six dimensions into a vector of magnitude  $1/\sqrt{2}$  in the three-dimensional spaces. There are also some permutations of rows and columns, but these are immaterial.]

The analogue for the projection from six dimensions to three of the finite-width band in the case of projection from two dimensions to one is the projection of a point from the six-dimensional space into the complementary three-dimensional space defined by the lower half of the matrix and the determination of whether this point is or is not within

some finite-sized region. Points that project within that region are then projected from six-dimensional space into the direct three-dimensional space using the top half of the matrix. The exact size and shape of the appropriate region used to define the band present problems that are discussed below, but, as in the two-to-one case, the density of the resulting 'quasilattice' is proportional to the volume of the selection region, which conveys additional information. Fig. 4 shows a portion of a three-dimensional array of points generated by this procedure projected into two dimensions along a fivefold axis. Like the vertices of the Penrose tiles, the points in this pattern lie on families of parallel lines, the projections of parallel planes, with spacings in the ratio of 1 to  $\tau$ .

Because the six-dimensional lattice is hypercubic, its reciprocal lattice is also hypercubic, and it projects, again using the upper and lower halves of matrix  $P$ , into two mutually orthogonal three-dimensional reciprocal lattices. A vector  $\mathbf{h}$  of magnitude  $1/d$  in the direct reciprocal space will be perpendicular to a family of planes in direct real space with corresponding average spacing  $d$ . Because  $\exp(2\pi i \mathbf{h} \cdot \mathbf{r})$  has constant values on these planes, the diffracted intensity depends only on the projection of the planes onto the reciprocal-lattice vector, and the Fourier transform of the three-dimensional quasilattice can be reduced directly to the two-to-one dimensional problem, as may be seen as follows:

An infinite set of six-dimensional reciprocal-lattice points will project onto the same radial line in each of the three-dimensional spaces. Because the spaces are mutually orthogonal, unit vectors along these lines form an orthonormal basis for a two-dimensional section through the six-dimensional space, and, in general, points that lie in this plane may be represented by linear combinations, with integral coefficients,

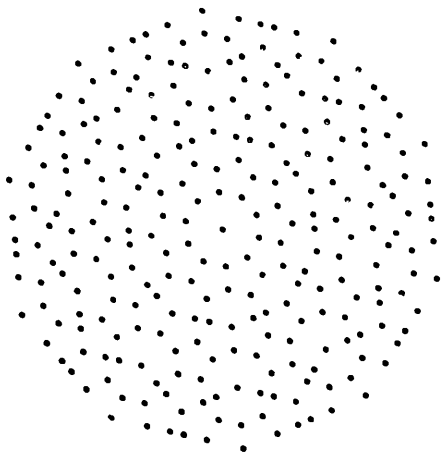


Fig. 4. A region of a three-dimensional projection of a 'band' in six-dimensional space, projected in turn into two dimensions along a fivefold axis. Families of parallel planes with quasi-periodic spacing are apparent.

of only two independent integers. For example, all points with indices of the form  $(m_1, 0, m_2, -m_1, 0, m_2)$  will project onto the line  $[1, 0, 0]$  in both spaces. The point  $(100\bar{1}00)$  has coordinates  $(2\alpha, 2\alpha\tau)$  in the section, whereas  $(001001)$  has coordinates  $(2\alpha\tau, -2\alpha)$ . A two-dimensional lattice based on these two displacement vectors and integral values of  $m_1$  and  $m_2$  will be a square lattice of exactly the type considered earlier (Fig. 2). Similarly, all points with indices of the form  $(m_1, m_2, m_2, -m_2, m_2)$  project onto the line  $[\tau, 1, 0]$  in the direct space and the line  $[\tau, 1, 0]$  in the complementary space. The point  $(100000)$  has coordinates  $(1, 1)$  in the plane defined by these vectors, whereas  $(0111\bar{1}1)$  has coordinates  $(\sqrt{5}, -\sqrt{5})$ , so that a lattice based on these vectors is a rectangular lattice whose unit-cell edges make  $45^\circ$  angles with the coordinate axes and have an axial ratio of  $1:\sqrt{5}$ .

The general procedure for the generation of a diffraction pattern is then, for any direction in reciprocal space into which a vector in six-dimensional space with integral indices projects, to construct a two-dimensional lattice in which the coordinates are the displacements along that direction in the direct and complementary spaces. In real space, there will be families of parallel planes projecting onto the reciprocal-lattice vector with average spacing  $d = a/r_x$ , where  $a$  is a cell edge, and the projection points will fall within a slice of thickness  $t = (r_y/r_x)w$ , where  $w$  is now the diameter of the selection region in that direction. Again, the intensity is proportional to  $\sin^2(\pi t/d)/(\pi t/d)^2 = \sin^2(\pi r_y w)/(\pi r_x w)^2$ . For convenience we shall follow Cahn, Shechtman & Gratias (1986) and transform the six-dimensional indices  $n_1$  to  $n_6$  into indices related to a three-dimensional cubic lattice. The indices take the form  $h + h'\tau$ ,  $k + k'\tau$ ,  $l + l'\tau$ , where  $h = n_1 - n_4$ ,  $h' = n_3 + n_6$ ,  $k = n_2 - n_5$ ,  $k' = n_1 + n_4$ ,  $l = n_3 - n_6$  and  $l' = n_2 + n_5$ . Because the  $n_i$  are integers, there is a selection rule that  $h + k'$ ,  $k + l'$  and  $l + h'$  must all be even. Using these indices, we get  $r_x^2 = [(h + h'\tau)^2 + (k + k'\tau)^2 + (l + l'\tau)^2]/a^2$  and  $r_y^2 = [(h' - h\tau)^2 + (k' - k\tau)^2 + (l' - l\tau)^2]/a^2$ .

It is apparent that, for there to be a strong diffraction spot,  $r_y w$  must be less than 1, and if  $w$  and  $a$  are comparable in magnitude,  $r_y$  should then be as small as possible. This occurs when the pairs  $h$  and  $h'$ ,  $k$  and  $k'$  and  $l$  and  $l'$  all have the form  $mF_n$  and  $mF_{n+1}$ ,  $m$  is as small as possible, and  $n$  is positive. Fig. 5 is a reproduction of a portion of an electron diffraction photograph taken from a rapidly solidified Mn-Al sample looking down a twofold axis, with indices of the prominent rows marked along the margin in the notation of Cahn, Shechtman & Gratias (1986). All diffraction spots in this view have indices of the form  $h/h'$ ,  $k/k'$ ,  $0/0$ , and the parity selection rule requires that  $h'$  and  $k$  be even. Several significant features may be observed in this pattern. There are several prominent rows radiating from the origin at  $(0/0, 0/0)$  in

the lower left-hand corner. The horizontal and vertical radial rows have spots with increasing intensity as the radius increases by successive factors of  $\tau$ , in a pattern that strongly resembles that in Fig. 1. Two radial rows making angles of  $\arctan(1/\tau)$  and  $\arctan \tau$  are very different. The row at  $\arctan \tau$  has two bright spots at radii related by a factor of  $\tau^3$ , and the outer bright spot is flanked by much weaker spots at radii related by a factor of  $\tau$ . In the row at  $\arctan(1/\tau)$  the bright spots are missing. Fig. 6 shows the two-dimensional lattices corresponding to these rows. The lattice for the  $\arctan \tau$  row contains all points, whereas that for the  $\arctan(1/\tau)$  row contains only those that are filled in. Both lattices are rectangular, with axial ratios of  $1:\sqrt{5}$ , but the one for the  $\arctan(1/\tau)$  row has both cell edges twice as long, and it is centered. The lattice points corresponding to the four spots on the  $\arctan \tau$  row are circled; the two closest to the horizontal axis, corresponding to high intensity, belong only to that row, but the others belong to both rows.

It should be noted that the indices given here imply structural units that are larger than those implied by the indices assigned by Cahn, Shechtman & Gratias (1986) by a factor of  $\tau^3$ . This is because if  $a$ , the edge of the basic rhombus in projection, and  $w$ , the diameter of the selection region in the complementary space, are of comparable magnitudes, the intensity formula predicts an extremely weak intensity for the reflection indexed as  $1/0, 0/1, 0/0$ , whereas the reflection to which they have assigned these indices is rather strong. The indexing scheme of Cahn, Shechtman & Gratias (1986) can be reconciled with the intensity formula if a much smaller selection region is chosen, leading to a much lower density of the projected quasilattice. Calculations (Cahn & Gratias, 1986) of neutron intensities (Mozer, Cahn, Gratias & Shechtman, 1986) on a model for the alloy indicate that this may indeed be appropriate.

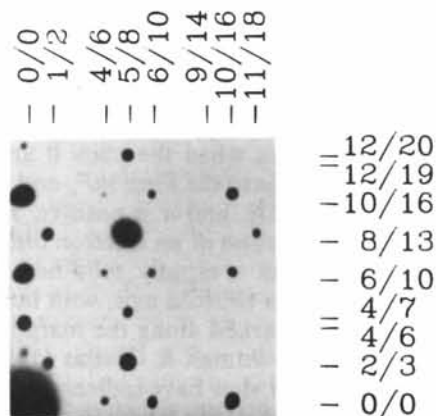


Fig. 5. A portion of the electron diffraction pattern of the icosahedral phase of Mn-Al along a twofold axis. Rows are indexed  $h/h', k/k'$ , where  $(d^*)^2 = (a^*)^2[(h+h'\tau)^2 + (k+k'\tau)^2]$ .

### Real-space structures

Although there is some controversy (Pauling, 1985; Carr, 1986; Cahn, Gratias & Shechtman, 1986; Mackay, 1986; Bancel, Heiney, Stephens & Goldman, 1986) over what sort of structure the rapidly solidified alloy of aluminium and manganese actually has, and it is not clear that the three-dimensional tiling is the best way to describe the structure, a structure can be constructed with tiles that produces a diffraction pattern with icosahedral symmetry. Such a structure must satisfy certain conditions, which we shall discuss in this section.

In generating a one-dimensional non-periodic sequence of line segments with lengths 1 and  $\tau$ , the procedure uses a two-dimensional lattice oriented at the irrational angle  $\arctan(1/\tau)$  and projects those lattice points that lie within a band of width  $1+\tau$  into the one-dimensional space. This appears to be a 'natural' width because it results in two, and only two, lengths of line segment. It is also the projection of the unit square into the complementary space. In their consideration of projection from six dimensions into three, Duneau & Katz (1985) appear to have assumed that an equally 'natural' choice of the selection region would be the projection of the six-dimensional unit hypercube, which is a triacontahedron - a figure with thirty faces, each a rhombus with an acute angle of  $2 \arctan(1/\tau) = 63.4^\circ$ . Elser (1986) has discussed the diffraction pattern that results from use of this selection region. The generalization of his procedure to selection regions of more complex shapes is not at all straightforward. As long as the study remains purely mathematical, the use of the

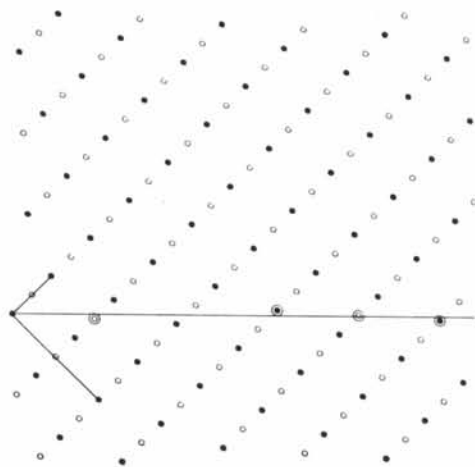


Fig. 6. Two-dimensional lattice formed by projection from six dimensions into two orthogonal one-dimensional spaces. Points close to the horizontal line correspond to the reciprocal-quasilattice points for strong reflections. All points in this section contribute to spots along the radial line at  $\arctan \tau$  from the horizontal in Fig. 5, but only the filled ones contribute on the line at  $\arctan(1/\tau)$ .

tricontahedron seems to be a reasonable assumption, but as soon as attempts are made to describe a plausible atomic structure for a real object having these diffraction properties, serious problems arise that may be classified in two (not entirely unrelated) categories, density and connectivity.

In order to propose a long-range-ordered structure for a quasicrystal, it is necessary to fit the required number of atoms into a set of blocks that are convex polyhedra that can be packed to fill space with the proper set of interatomic vectors. Mackay (1981, 1982) has shown that such a structure can be constructed using two rhombohedra whose faces are  $63.4^\circ$  rhombuses, a pointed one with the acute angles meeting at the threefold axis and a flat one with the obtuse angles meeting at a threefold axis. [Baer (1970) showed a similar result in an entirely different context.] These objects have volumes in the ratio  $\tau:1$ , and they also occur in the number ratio  $\tau:1$  (Levine & Steinhardt, 1984), as in one and two dimensions. Because all unit vectors along coordinate axes in six dimensions project onto unit vectors along fivefold directions in three dimensions, any subset of three of the six coordinate axes in six dimensions will project into one or the other of the rhombohedra. However, the projection procedure generates an array of points that possess icosahedral symmetry over arbitrarily large finite regions, but it is impossible with the two rhombohedra alone to construct an object any larger than the one constructed from twenty of the acute rhombohedra that has this symmetry (except for one that consists entirely of acute rhombohedra, producing a 20-fold twin that does not have the quasicrystal diffraction pattern). The use of the Duneau & Katz (1985) triacontahedron achieves icosahedral symmetry by superposing distinct tilings related to one another by rotations or reflections, leading to extensive interpenetration of the two rhombohedral shapes.

Interpenetration can be prevented by forbidding the use of the obtuse rhombohedron, which in turn can be achieved by using as the selection region a regular icosahedron with opposite faces separated by the length of the long diagonal of the acute rhombohedron. While this figure eliminates the interpenetrations, it introduces a new problem. Points that project into the vicinity of a vertex of the icosahedron in complementary space will have three or fewer neighbors in direct space, leading to dangling bonds or enclosed regions that are not convex.

The interpenetration and dangling-bond problems can apparently be simultaneously eliminated by using as the selection region a reentrant figure that is the union of an icosahedron and a regular dodecahedron that together have the same vertices as the triacontahedron. If this figure is used there are no pairs of obtuse rhombohedra sharing faces, but two new solids appear in the set that is required to fill direct three-dimensional space. One is a rhombic dodecahedron

(distinct from the classic cubic form commonly given this designation), a figure having twelve rhombus-shaped faces, a volume of  $2\tau$  times the volume of an acute rhombohedron, and symmetry  $mmm$ . The other is a rhombic icosahedron, a figure with twenty faces, a volume  $5\tau$  times the volume of the acute rhombohedron, and symmetry  $\bar{5}m$ . The dodecahedron can be tiled with two acute rhombohedra and two obtuse rhombohedra in a configuration that has symmetry  $mm2$  in two distinct ways. If the selection region is the triacontahedron of Duneau & Katz (1985) the internal quasilattice nodes required by both orientations are generated, leading to interpenetration and consequently a much larger number of distinct tiles. Similarly, the icosahedron can be tiled with five acute and five obtuse rhombohedra in ten different ways, with the Duneau & Katz (1985) procedure generating the internal nodes required by all of them.

If an atomic structure is to be constructed from a set of units having identical faces, atoms that cross the boundary between adjacent units must match, so that the arrangements of atoms in these faces must also be identical, at least to first order. The cell edge of f.c.c. aluminium metal is a little more than  $4.0 \text{ \AA}$  long, implying a volume per atom of about  $16 \text{ \AA}^3$ . A manganese atom is somewhat smaller than this. A real structure cannot have a density that is higher than that implied by these values by more than a few percent. The icosahedral diffraction patterns from the aluminium-manganese alloy, if the indexing scheme of Cahn, Shechtman & Gratias (1986) is used, imply that the edge of the basic rhombus is about  $4.63 \text{ \AA}$ , which gives the obtuse rhombohedron a volume of about  $46 \text{ \AA}^3$  and the acute one a volume of about  $75 \text{ \AA}^3$ . The obtuse rhombohedron therefore has room for three atoms and the acute one for five. Firstly, for the obtuse rhombohedron, three atoms can be accommodated by placing them either at the centers of the edges or at the centers of the faces. Atoms cannot occupy the vertices, because that accounts for only one atom and there is no other site where atoms can be placed that does not have multiplicity three except along the short diagonal, where there is insufficient room for two more atoms. There are sites in the quasilattice at which 20 of the acute rhombohedra meet at a point, and atoms at the centers of the faces would lead to a cluster of thirty aluminium atoms surrounding a large void, a configuration that seems unlikely. Atoms at the centers of the edges lead to a cluster of 12 atoms around a smaller void, a configuration that has been observed in alloy systems. Atoms at the centers of the edges account for three of the five atoms the acute rhombohedron can accommodate. The other two may be fitted into nine-coordinated holes in the interior. One or both may be manganese. The dodecahedral unit has room for 16 atoms, of which eight are located on the edges of the surface rhombuses. The rhombic icosahedron

has space for 40 atoms, of which 15 are on the surface.

It should be noted that it is not necessary for an actual structure to have icosahedral symmetry over extended regions. It is only necessary that its set of interatomic vectors have that symmetry. The icosahedral diffraction pattern could therefore be produced by a packing of the two rhombohedral shapes alone. However, because there is insufficient space for a manganese atom in the obtuse rhombohedron, there would be only one type of local environment for a manganese atom, contrary to observations by Mössbauer spectroscopy (Swartzendruber, Shechtman, Bendersky & Cahn, 1985) and EXAFS (Stern, Ma & Bouldin, 1985) that there must be at least two distinct transition-metal sites. Although it is possible that required differences can result from more distant neighbors owing to the different types of packing, it would appear that a satisfactory structure for the aluminium-manganese and other quasicrystalline alloys is likely to contain units based on one or both of the larger solids. In particular, it may be possible to fill space with the acute rhombohedron and the rhombic icosahedron, which between them possess all the necessary convex vertices.

The indexing scheme assigned in this paper implies an edge for the basic rhombus that is larger by a factor of  $\tau^3$ , or about 19.6 Å. Unit cells of that size are not unusual in the Mn-Al system, and this cell volume allows ample room for multiple formula units, making the problem of density adjustment much easier. Moreover, the quasilattice generated by the projection process has the property that if the selection region is contracted by a factor of  $\tau^3$  the resultant quasilattice is identical to the original one except that it is expanded by a factor of  $\tau^3$ . Therefore a large structure can be constructed from the smaller blocks. There is no absolute criterion for choosing the size of a fundamental unit. It is chosen here on the basis of the transition from low diffracted intensity to high diffracted intensity.

Regardless of the size of the selection region, the formula given in this paper provides a means of computing the lattice part of the Fourier transform. If the selection region has icosahedral symmetry and is convex, the diameter in different directions cannot vary greatly, so that for practical purposes it can probably be adequately approximated by a sphere whose radius could be a parameter in a refinement

procedure. On the other hand, if the region is not convex there will be differences in the intensities of reflections at the same reciprocal-lattice radii in different directions. In cases where reflections at the same radius along different lines in the electron diffraction pattern have different intensities, therefore, these differences may be ascribed either to the effects of different quasilattice weighting or to the effects of atomic arrangement.

The author gratefully acknowledges interesting and helpful discussions with N. F. Berk, J. W. Cahn, H. A. Fowler, D. Gratias and B. Mozer. He also wishes to thank C. B. Shoemaker and D. P. Shoemaker for a critical reading of an earlier draft of the manuscript and many constructive comments.

#### References

- BAER, S. (1970). *Zome Primer*. Albuquerque: Zomeworks Corp.
- BANCEL, P. A., HEINEY, P. A., STEPHENS, P. W. & GOLDMAN, A. J. (1986). *Nature (London)*, **319**, 104.
- BENDERSKY, L. (1985). *Phys. Rev. Lett.* **55**, 1461-1463.
- BRUIJN, N. G. DE (1981). *Proc. K. Ned. Akad. Wet. Ser. A*, **43**, 39-52, 53-66.
- CAHN, J. W. & GRATIAS, D. (1986) *J. Phys. (Paris) Colloq.* **47**, C3-415-424.
- CAHN, J. W., GRATIAS, D. & SHECHTMAN, D. (1986). *Nature (London)*, **319**, 102-103.
- CAHN, J. W., SHECHTMAN, D. & GRATIAS, D. (1986). *J. Mater. Res.* **1**, 13-26.
- CARR, M. J. (1986). *J. Appl. Phys.* **59**, 1063-1067.
- DUNEAU, M. & KATZ, A. (1985). *Phys. Rev. Lett.* **54**, 2688-2691.
- ELSER, V. (1986). *Acta Cryst.* **A42**, 36-43.
- GARDNER, M. (1977). *Sci. Am.* **236**, 110-121.
- KALUGIN, P. A., KITAYEV, A. YU. & LEVITOV, L. S. (1985). *J. Phys. (Paris) Lett.* **46**, L601-L607.
- KRAMER, P. & NERI, R. (1984). *Acta Cryst.* **A40**, 580-587.
- LEVINE, D. & STEINHARDT, P. J. (1984). *Phys. Rev. Lett.* **53**, 2477-2480.
- MACKAY, A. L. (1976). *Phys. Bull.* 495-497.
- MACKAY, A. L. (1981). *Sov. Phys. Crystallogr.* **26**, 517-522.
- MACKAY, A. L. (1982). *Physica (Utrecht)*, **114A**, 609-613.
- MACKAY, A. L. (1986). *Nature (London)*, **319**, 103-104.
- MOZER, B., CAHN, J. W., GRATIAS, D. & SHECHTMAN, D. (1986). *J. Phys. (Paris) Colloq.* **47**, C3-350-360.
- PAULING, L. (1985). *Nature (London)*, **317**, 512-514.
- PENROSE, R. (1974). *Bull. Inst. Math. Appl.* **10**, 266-271.
- SHECHTMAN, D., BLECH, I., GRATIAS, D. & CAHN, J. W. (1984). *Phys. Rev. Lett.* **53**, 1951-1953.
- STERN, E. A., MA, Y. & BOULDIN, C. E. (1985). *Phys. Rev. Lett.* **55**, 2883-2886.
- SWARTZENDRUBER, L., SHECHTMAN, D., BENDERSKY, L. & CAHN, J. W. (1985). *Phys. Rev. B*, **32**, 1383-1385.
- ZIA, R. K. P. & DALLAS, W. J. (1985). *J. Phys. A*, **18**, L341-L345.